An HI interstellar bubble surrounding WR 85 and RCW 118

J. Vasquez[1]⋆, C. Cappa[1,2]† and N.M. McClure-Griffiths[3]

[1] *Instituto Argentino de Radioastronomía, C.C.5. 1894, Villa Elisa, Argentina*
[2] *Facultad de Ciencias Astronómicas y Geofísicas, Universidad Nacional de La Plata, La Plata, Argentina*
[3] *Australia Telescope National Facility, CSIRO; P.O. Box 76, Epping NSW 1710, Australia*

ABSTRACT

We analyze the distribution of the interstellar matter in the environs of the Wolf-Rayet star LSS 3982 (= WR 85, WN6+OB?) linked to the optical ring nebula RCW 118. Our study is based on neutral hydrogen 21cm-line data belonging to the Southern Galactic Plane Survey (SGPS).

The analysis of the HI data allowed the identification of a neutral hydrogen interstellar bubble related to WR 85 and the 25′-diameter ring nebula RCW 118. The HI bubble was detected at a systemic velocity of –21.5 km s^{-1}, corresponding to a kinematical distance of 2.8±1.1 kpc, compatible with the stellar distance. The neutral stucture is about 25′ in radius or 21±8 pc, and is expanding at 9±2 km s^{-1}. The associated ionized and neutral masses amount to 3000 $M_{\odot}$. The CO emission distribution depicts a region lacking CO coincident in position and velocity with the HI structure. The 9′.3-diameter inner optical nebula appears to be related to the approaching part of the neutral atomic shell. The HI void and shell are the neutral gas counterparts of the optical bubble and have very probably originated in the action of the strong stellar wind of the central star during the O-type and WR phases on the surrounding interstellar medium. The HI bubble appears to be in the momentun conserving stage.

Key words: ISM: bubbles – stars: Wolf-Rayet – ISM: HII regions

1 INTRODUCTION

Wolf-Rayet (WR) stars are the evolutionary descendents of massive O-type stars. With mass loss rates in the interval (1-5)×10^{-5} M$_{\odot}$ yr^{-1} and terminal velocities of 1000 - 3000 km s^{-1} (van der Hucht 2001; Cappa et al. 2004), these hot and luminous stars are one of the most powerful stellar wind sources in our Galaxy. Of-type stars are also characterized by high mass loss rates and terminal velocities (Lamers & Leitherer 1993; Prinja, Barlow & Howarth 1990).

The mechanical energy released to the interstellar medium (ISM) during the WR phase only ($t_{WR} \lesssim 7 \times 10^5$ yr, Meynet & Maeder 2003) is in the range (1-30)×10^{50} erg, comparable to the mechanical energy injected during a supernova explosion. Both the mass flow from the WR star and the previous O-type star phases strongly modify the energetics, the morphology and the chemical abundances of the ISM in the environs of the star.

The interaction of the strong stellar winds with the surrounding interestellar matter has been analyzed by several authors, taking into account different enviroments (e.g. García-Segura & Mac Low 1995). The stellar flow sweeps up the surrounding material creating *interstellar bubbles*, which are detected at different wavelengths from the UV to the radio range. In the optical regime, these structures are generally observed as filamentary ring nebulae in the light of Hα and [OIII] (e.g. Chu et al. 1983; Marston et al. 1994). They are related to many WR stars and to a relatively large number of O and Of stars. Shell-shaped structures created by stellar winds from massive stars are also identified in the far infrared and in the thermal radio continuum emission (e.g. Mathis et al. 1992; Cappa, Goss & Pineault 2002).

Interstellar bubbles appear as cavities and expanding shells in the neutral hydrogen 21cm line emission distribution (e.g. Cappa et al. 2003 and references therein). HI bubbles are external to their optical and radio continuum counterparts, and expand at relatively low velocities ($\lesssim 10$ km s^{-1}). In most of the cases the derived dynamical ages are larger than the duration of the WR phase, suggesting that the stellar winds of the massive O-type star progenitor has also contributed to creating the structures.

As part of a systematic search for neutral gas bubbles

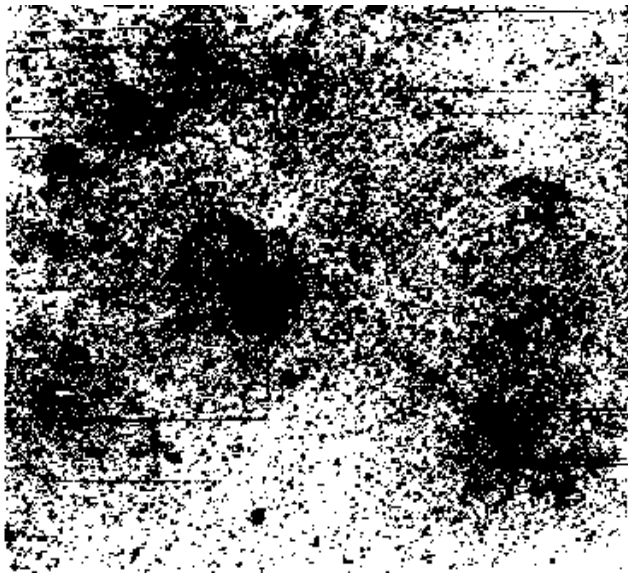**Figure 1.** Hα image in (α, δ) coordinates showing the two concentic rings around WR 85 (taken from Marston et al. 1994). North is up and East is to the left.

around massive stars, we present here a study of the ISM surrounding WR 85 (= HD 155603B = LSS 3982) based mainly on H I 21cm-line data belonging to the Southern Galactic Plane Survey (SGPS) and additional molecular and radio continuum data.

WR 85 is classified as WN6h + OB?. Different distance estimates have been published for this star. WR 85 belongs to the HD 155603 group, for which Moffat & FitzGerald (1977) find a distance of 1.8 kpc. Conti & Vacca (1990) and van der Hucht (2001) locate the star at d = 3.7±1.3 and 4.7±2.3 kpc, respectively, while Hipparcos measurements indicate 1.7 kpc. The X-ray point like source 1 WGA J1714.4-3949 coincides in position with the WR star (Pfeffermann & Aschenbach 1996).

HD 155603B is associated with the optical ring nebula RCW 118, of about $25'$ in diameter (Chu & Treffers 1981; Heckathorn, Bruhweiler & Gull 1982, Marston et al. 1994; Marston et al. 1994b). Chu et al. 1983 observed RCW 118 with the Curtis-Schmidt-0.6m telescope at CTIO in Hα, [OIII]λ5007 and [SII]λ6730. These authors found that the ionized gas in the nebula has a LSR velocity of –15 km s^{-1}, and derived an expansion velocity $\leqq$ 10 km s^{-1} and a dynamical age of 6.7×10^5 yr, compatible with the duration of the WR phase. Based on the velocity of the ionized gas and on standard galactic rotation models, they estimated a kinematical distance d$_k \sim$ 2.3 kpc.

Marston et al. (1994) reobserved the nebula using the same telescope. Their Hα image reveals the presence of two semi-circular rings. The inner ring has a diameter of $9'.3$ and is centered on the WR star, whereas the outer one, $25'$ in diameter, is centered slightly to the south and south-east of the star. The two concentric structures can be clearly identified in the Hα image displayed in Figure 1.

RCW 118 is in the same line of sight to the SNR G347.3–0.5, discovered in the ROSAT All Sky Survey (RASS) by Pfeffermann & Aschenbach (1996). This SNR, 1° in diameter, is located at $\approx$ 6 kpc (see Lazendic et al. 2004).

Table 1. H I data: main observational parameters

(l,b) center	347°14′, –0°29′
Velocity range	–204, 124 km s^{-1}
Velocity resolution	1.64 km s^{-1}
Surveyed area	2°×2°
RMS noise	1.3 K
Synthesized beam	2′.6×2′.1

2 DATABASES

The H I 21cm-line emission data used in this paper belong to the Southern Galactic Plane Survey (SGPS) (McClure-Griffiths et al. 2005) obtained with the Autralia Telescope Compact Array (ATCA) and the Parkes radiotelescope (short spacing information). The H I data cube is centered at $(l, b, v) = (347°14', –0°29', –40$ km s^{-1}), covers a region of about 2°×2° around the WR star, and has a synthesized beam of 2′.6×2′.1. To improve the S/N ratio we applied a Hanning smoothing to the individual line images. Consequently, the original rms noise level of 2.4 K was lowered to 1.3 K and the channel velocity resolution was doubled. The main observational parameters of the final data cube are summarized in Table 1.

Additional infrared, radio continuum and molecular data were also analyzed. High resolution infrared images (HIRES) were obtained from IPAC[1]. The IRAS data, obtained at 12, 25, 60 and 100μm, have angular resolutions in the range 0′.5 to about 2′. Radio continuum data at 2.4 GHz were obtained from the survey by Duncan et al. (1995) with an angular resolution of 10′.4. The molecular data corresponds to the CO (J = 1→0) line at 115 GHz and belong to the CO survey by Dame et al. (2001), with angular and velocity resolutions of 9′and 1.3 km s^{-1}, respectively, and a rms noise of 0.3 K.

3 IONIZED AND NEUTRAL GAS DISTRIBUTION TOWARDS WR 85

3.1 H I line emission distribution

The strong stellar winds from massive stars are expected to sweep-up the interstellar material around the wind source and to create a highly evacuated region surrounded by an expanding shell. If the ionizing front is trapped within the envelope, the void and the surrounding shell are expected to appear as a region lacking neutral material encircled by regions of enhanced H I emission. The analysis of the neutral gas emission distribution in the environs of these stars allows identification of such cavities and surrounding shells associated with the wind sources.

The criteria adopted to relate an H I cavity and shell to a certain star are: (i) the star should be located close to the centre of the void or within the inner border of the H I surrounding shell; (ii) the ionized ring nebula, if present, should appear projected within the cavity or close to the inner border of the neutral shell; and (iii) the kinematical

---

[1] IPAC is fouded by NASA as part of the IRAS extended mission under contract to Jet Propulsion Laboratory (JPL) and California Intitute of Technology (Caltech).

distance to the H I structure should be compatible, within errors, with the stellar distance.

To facilitate the visualization of the general characteristics of the H I emission in the line of sight to this region of the Galaxy, we show the average H I profile corresponding to an area of $1° \times 1°$ centered at the position of WR 85 in the top panel of Figure 2. The bottom panel shows a plot of the kinematical distance d_k *versus* the LSR radial velocity for the galactic longitude $l = 347°$, as obtained from the circular galactic rotation model by Brand & Blitz (1993)

Brightness temperatures higher than a few K are observed for velocities spanning the range –130 to +50 km s^{-1}. According to the quoted circular galactic rotation model, gas at negative velocities is placed at kinematical distances $d_k \approx 0-7$ kpc or $d_k \geqq 9$ kpc, while positive velocities are forbidden for distances closer than 17 kpc. Gas within the near distance range is most probably related to the Local and the Carina-Sagittarius arms (Georgelin & Georgelin 1976).

To analyze in some detail the neutral atomic gas distribution in the environs of the WR star, we obtained a series of H I line images at constant velocities, paying particular attention to the gas distribution at negative velocities. The analysis of the neutral atomic gas distribution within the velocity range –150 to 0 km s^{-1} shows a clear void with the star projected close to its centre at velocities of about –21 km s^{-1}.

The top panel of Figure 3 displays the H I column density distribution within the velociy interval –28.0 to –16.5 km s^{-1}, where the void clearly detected. The void appears surrounded by an almost circular shell. The centroid of the structure, defined following the maxima in the shell, is placed at $(l, b) = (347°26', -0°37')$, close to the position of WR 85 (indicated by the star symbol). The brightness temperature gradient of the structure is slightly steeper towards the galactic plane than towards the other sections of the shell, indicating the presence of higher density regions close to $b = 0°$.

The bottom panel of Fig. 3 displays a superposition of the Hα image of the region obtained from the Southern H-alpha Sky Survey Atlas (SHASSA) (Gaustad et al. 2001) (*greyscale*) and the same H I contours of the top panel. The $25'$-diameter outer nebula is clearly detected in the optical image (see Fig. 1 for a comparison), while the $9.'3$ -diameter inner nebula is barely identified. The bottom panel of Fig. 3 shows that the $25'$-diameter optical nebula is projected onto the H I cavity and close to the inner border of the H I shell.

The systemic velocity of the structure, defined as the velocity at which the H I cavity presents its largest dimensions and deepest temperature gradient, is $v_{sys} \approx -21$ km s^{-1}. This value is compatible, within errors, with the velocity of the ionized gas found by Chu & Treffers (1981) (–15 km s^{-1}).

The presence of the outer optical nebula close to the inner border of the H I shell and the morphological agreement between the RCW 118 and the H I emission, along with the agreement between the systemic velocity of the H I structure and the velocity of the ionized gas indicate that the H I feature is related to RCW 118.

Figure 4 displays two profiles showing the H I column density *versus* the galactic longitude for $b = -0°36'$ (*thin line*) and the galactic latitude for $l = 347°25'$ (*thick line*).
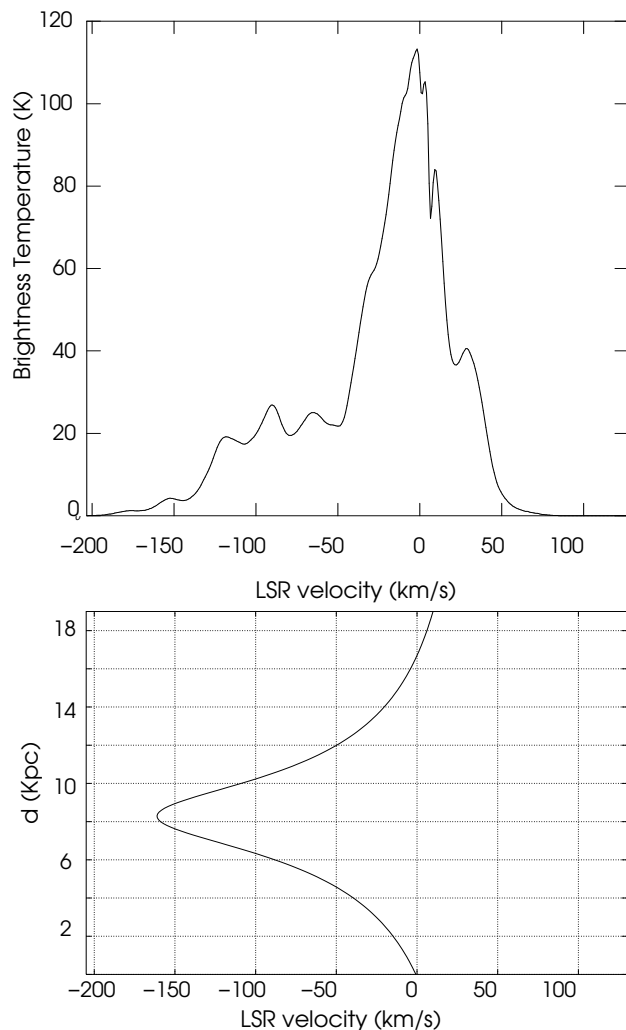

Figure 2. *Top panel:* Average H I brightness temperature spectrum *versus* LSR velocity, corresponding to an area of $1° \times 1°$ centered at the position of WR 85. *Bottom panel:* Kinematical distance *versus* LSR velocity plot obtained from the analytical fit to the circular galactic rotation model by Brand & Blitz (1993) for $l = 347°$.

This plot clearly shows that the WR star is projected onto a minimun in the H I emission distribution. The neutral shell is identified with arrows. The wide line shows that although most of the neutral gas near $b = 0°$ is linked to the Sagittarius arm, it is unconnected to the H I feature shown in Fig 3.

We analyzed is some detail the H I gas distribution in the close environs of the $9.'3$ optical ring. The top panel of Fig. 5 displays the neutral gas emission distribution for the velocity interval –29.3 to –27.6 km s^{-1} (in grey scale and coutour lines), while the bottom panel shows an overlay of the optical image (grey scale) and the H I emission distribution (contour lines). The figure reveals the presence of neutral gas emission closely bordering the inner semi-circular optical ring. The morphological correlation between the H I emission and the border of the inner nebula suggests that the ionized and the neutral material are related. Some correlation between the inner optical ring and neutral hydrogen is also detected at velocities spanning the range –27.6 to –25.2 km s^{-1}. This
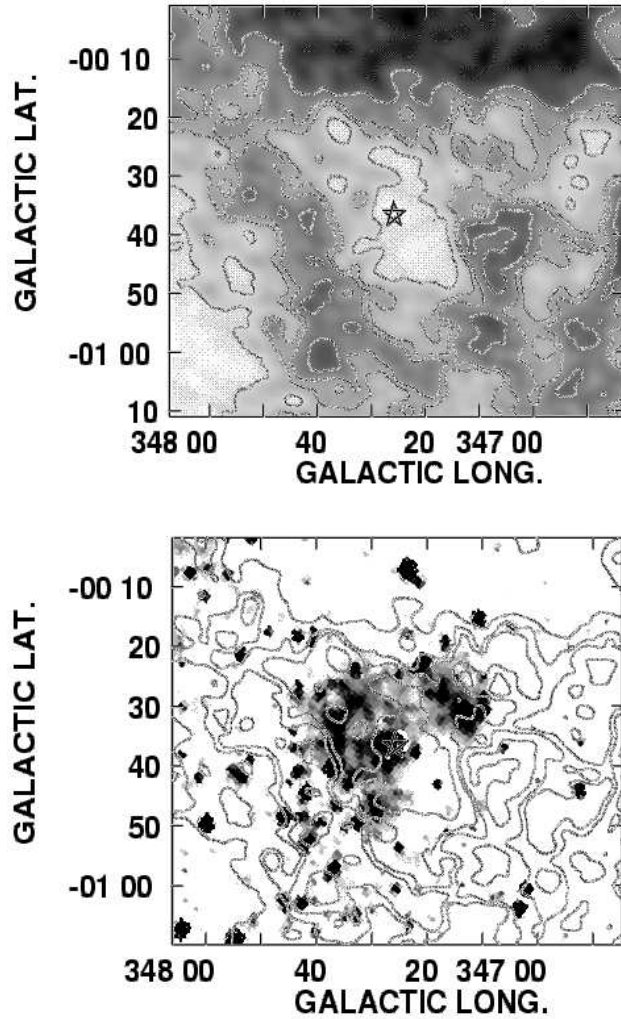
Figure 3. *Top panel:* H I column density distribution surrounding WR 85 within the velocity interval –28.0 to –16.5 km s^{-1}. The grayscale corresponds to $(1.2\text{-}1.7)\times10^{21}$ cm^{-2} and the contour lines are 1.2, 1.4, 1.5 and 1.6×10^{21} cm^{-2}. The star symbol indicates the position of the WR star. *Bottom panel:* Overlay of the SHASSA Hα image of the nebula and the same H I contours of the top panel. Hα units are arbitrary.

H I gas is also shown as the H I peaks interior to the H I shell detected about $10'$ far from the star in the profiles in Fig. 4.

The velocity interval at which the correlation between the inner ring and the H I cloud is better detected suggests that the inner optical nebula is located on the approaching section of the expanding shell associated with RCW 118.

3.2 Radio continuum emission

Figure 6 displays an overlay between the radio continuum emission at 2.4 GHz (contour lines) and the H I column density distribution (greyscale). Within the region of interest, the figure shows a radio source centered at $(l, b) = (347°32',$ $-0°29')$, coincident with the brightest section of RCW 118 and with the inner optical ring located close to the star. Weak radio emission can also be detected toward higher negative galactic latitudes and lower galactic longitudes, co-
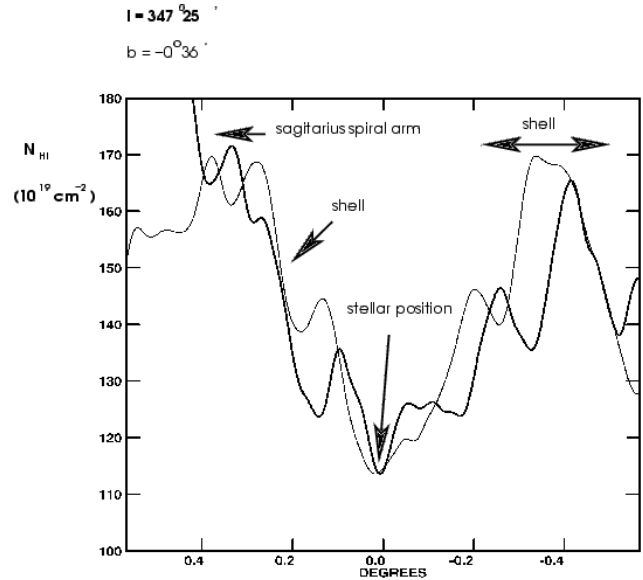

Figure 4. Profiles showing the H I column density within the velocity interval –28.0 to –16.5 km s^{-1} *versus* galactic longitude obtained at $b = -0°36'$ (thin line) and *versus* galactic latitude at $l = 347°25'$ (thick line). The x-axis is referred to the stellar position.

incident with fainter regions of RCW 118. The positional coincidence between both the radio source and the weak radio emission, and RCW 118 suggests that the emission at 2.4 GHz originates in the ionized nebular gas.

An image at 4.85 GHz can be obtained from the PMN Survey (Condon, Broderick & Seielstadet 1995). However, the presence of extended areas lacking radio data within the region of interest does not make this image useful. The presence of weak radio emission in this region is also evident at 4.85 GHz in the survey by Haynes, Caswell & Simonset (1978).

3.3 Molecular and IR emission

The left panel of Figure 7 shows the CO(J=1→0) line emission distribution within the velocity range –32.5 to –24.7 km s^{-1} taken from the Dame et al. (2001) survey. The stellar position is indicated by the star. A region of low molecular emission, $\sim 1°30'\times 0°45'$ in size, centered near $(347°25',$ $-0° 36')$ is evident in the image. The right panel of the figure displays an enlargement of the molecular void showing an overlay of the CO emission distribution (thick contour lines) and the H I column density image of Fig. 3 (grayscale and thin contour lines).

The image on the right shows the clear correspondence between the H I structure and the higher galactic longitude section of the CO cavity $(l > 347°00')$. Note that the CO maxima are external to the H I shell, suggesting that some stratification in the gas density is present. The section of the molecular cavity at $l < 347°00'$, which is wider in galactic latitude, is not linked to the interstellar bubble.

The HIRES IRAS images at 12, 25, 60 and 100 μm do not show any structure connected either to the optical or to the H I and CO shells. Only an IR emission gradient probably
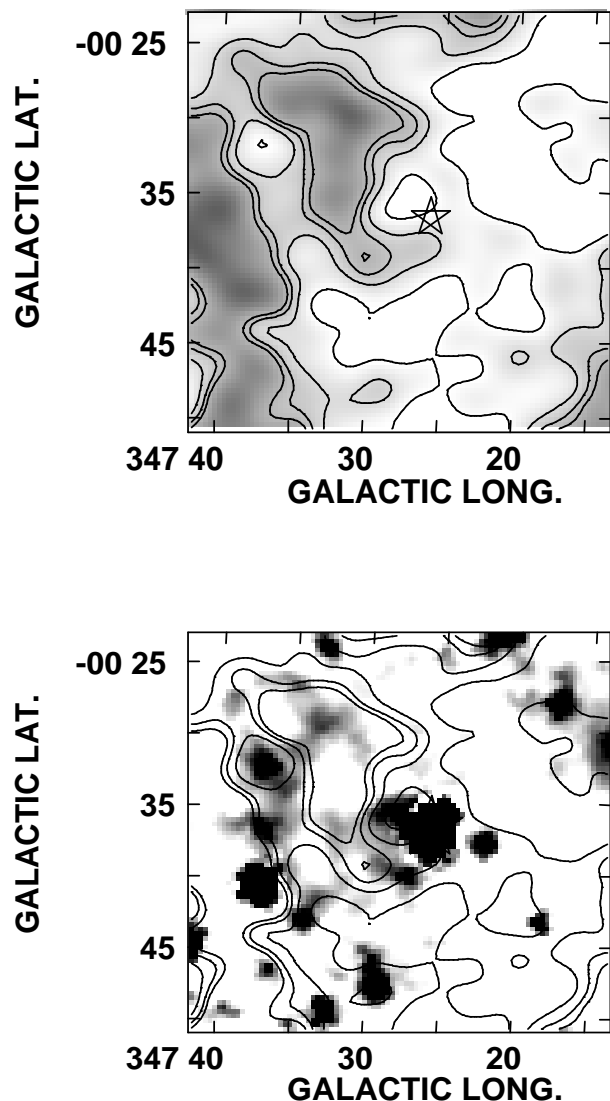
Figure 5. *Top panel:* HI emission distribution within the velocity interval –29.3 to –27.6 km s^{-1} in grey scale and contour lines. The grey scale corresponds to 45 to 90 K. The contour lines are 45, 50, 53, 55 K. The cross marks the position of the WR star. *Bottom panel:* Overlay of the SHASSA Hα image and the same HI contours of the top panel.

linked to the galactic plane is present in the images at 60 and 100 μm.
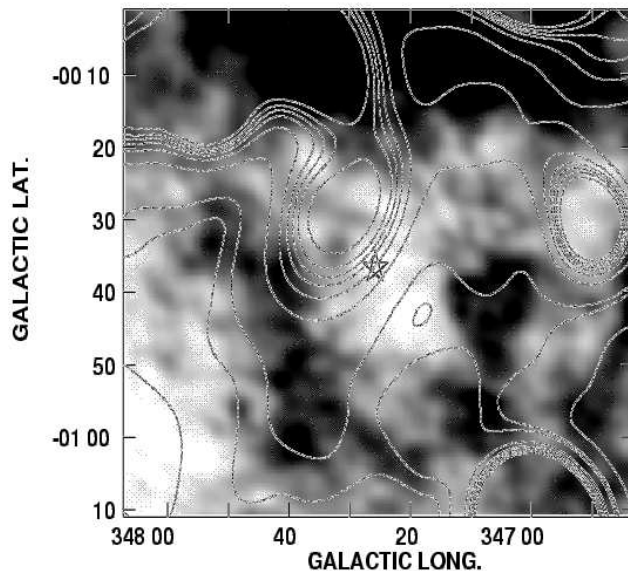

Figure 6. Overlay of the radio continuum image at 2.4 GHz (contour lines) and the HI column density distribution (grayscale). The star marks the position of WR 85. Contour lines are 0.04, 0.09, 0.1, 0.27, 0.29 and 0.32 Jy.

4 THE HI BUBBLE RELATED TO WR 85 AND RCW 118

4.1 The distance

The kinematical distance d_k to the HI structure was estimated from the analytical fit to the circular galactic rotation model Brand & Blitz (1993).

This model predicts that gas at $v_{sys} = -21$ km s^{-1} should be located at 2.7±0.7 kpc or 14±1 kpc. The uncertainties in the quoted values were estimated by assuming the presence of non-circular motions of ≈ 6 km s^{-1}. The near kinematical distance estimate is compatible with the kinematical distance of the ionized gas ($d_k = 2.0$ kpc) derived using the same model.

Bearing in mind the available photometric data for WR 85 and the intrinsic color and absolute magnitude corresponding to a WN 6 star from van der Hucht (2001), the spectrophotometric distance estimate is d $\approx$ 2.2±0.9 kpc, where the uncertainty in the stellar distance corresponds to the error in the absolute magnitude (±0.9 mag). This distance estimate is consistent with the near kinematical distance derived from HI data.

van der Hucht (2001) suggests the existence of an OB companion to WR 85. However, the absence of OB absorption lines in the spectrum of WR 85 (Gamen, private communication) suggests that the OB companion would be at least 2.5 mag weaker than the WR star. Consequently, a correction factor to the apparent magnitude of WR 85 has not been taken into account.

Bearing in mind these values and the distances derived by different authors (see §1), we adopted $d_k = 2.8$±1.1 kpc for both the optical and the HI structures. The uncertainty in the adopted distance is 40%.

The agreement in position, velocity and distance among the WR star, RCW 118 and the HI feature suggests that the HI structure is associated with the outer optical ring nebula.

Table 2. Physical parameters of the HI bubble

(l, b) centroid	$347°26', -0°37'$
Velocity range v_2, v_1(km s^{-1})	$-28.0, -16.5$
Systemic velocity (km s^{-1})	-21 ± 5
Expansion velocity (km s^{-1})	9 ± 2
Angular radius of the HI cavity	$20'$
Angular radius of the HI shell	$30'$
Angular radius of the HI bubble	$25'$
Adopted distance (kpc)	2.8 ± 1.1
Linear radius of the HI bubble (pc)	21 ± 8
HI mass deficiency of the cavity (M$_\odot$)	220 ± 170
HI mass in the shell ($M_\odot$)	830 ± 780
HI mass in the HI bubble (M$_\odot$)	530 ± 400
Swept-up neutral mass (M$_\odot$)	720 ± 570
Dynamical age (yr)	$(\sim 1.1 \pm 0.5) \times10^6$

The presence of a central star characterized by a strong mass flow inside the HI structure and the optical nebula suggests that the stellar wind of the WR star and its massive progenitor may have had an important role in shaping the nebula. We therefore interpret the HI structure as the neutral gas counterpart of the optical interstellar bubble.

4.2 Main parameters of the interstellar bubble around WR 85

The physical parameters of the HI bubble are summarized in Table 2. The centroid of the structure was defined taking into account the position of the maxima in the shell.

The velocity range corresponds to the velocity interval where the structure is detected. The systemic velocity was defined in §3.1 The expansion velocity was estimated as $v_{exp} = (v_2 - v_1)/2 + 1.6$ km s^{-1} and represents a lower limit to the true expansion velocity. The extra 1.6 km s^{-1} allows for the presence of HI in the undetected caps of the expanding shell. Because of its small column density, these caps are difficult to identify in the fore- and background emission.

The cavity was defined following the contour line corresponding to 1.4×10^{21} cm^{-2}(see Fig. 3). The angular radius of the shell corresponds approximately to the outer border of the envelope. It can be clearly established for $b < -0°25'$, while confussion with fore- and background gas precludes the identification of the shell near $b < -0°10'$. The size of the bubble was estimated through the maxima in the shell.

The HI mass deficiency in the cavity and the HI mass in the shell were obtained from the column density image shown in Fig. 3. The swept-up neutral mass associated with the HI bubble was derived as a mean value between the mass deficiency in the cavity and the mass in the shell assuming a 10% He abundance.

Bearing in mind an error of 40% in the adopted distance, uncertainties in radii and masses are about 40% and 80%, respectively.

Evolutionary models of interstellar bubbles allow an estimate of the dynamical age as $t_d = 0.50\times10^6 R/v_{exp}$ yr (McCray 1983), corresponding to the momentum conserving stage of an interestellar bubble, where R is the radius of the bubble (pc), v_{exp} is the expansion velocity (km s^{-1}) and the constant is the deceleration parameter, which corresponds to a mean value between the energy and the momentum conserving cases. The derived dynamical age $t_d =$

1.1×10^6 yr, is larger than the duration of the WN phase of a massive star ($t_{WN} = 0.3\times10^6$ yr for a rotating star of 40 M$_\odot$, Meynet & Maeder 2003) and suggests that the O-type star progenitor of the present WR star has contributed in the formation of the bubble.

A rough estimate of the ionized mass M_i and the electron density n_e related to RCW 118 were obtained from the radio continuum image at 2.4 GHz (Fig. 6) using the classical expressions by Mezger & Henderson (1967) for the case of a spherical HII region. We derived the flux density by assuming that the strong radio source at $347°32'$, $-0°29'$ and part of the weak radio emission towards higher negative galactic latitudes and lower galactic longitudes are related to RCW 118. For a flux density $S_{2.4} = 12$ Jy, and assuming an electron temperature of 10^4 K, and a filling factor $f = 0.35-0.45$, we derived $M_i = 2100 - 2400$ M$_\odot$ and $n_e = 13 - 15$ cm^{-3}. The filling factor was estimated from the optical image and corresponds to an ionized shell of about $13'$ in radius and $4'$ in thickness. We assume that about 50-70 % of the shell surface is covered by gas. Uncertainties in the ionized masses and electron densities are about 80%. We have also assumed that He is singly ionized.

Taking into account the neutral atomic and the ionized masses, the total mass in the interstellar bubble is $M_s \sim 3000$ M$_\odot$. The average ambient density estimated by distributing the total mass within a volume of 21 pc in radius is ~3 cm^{-3}.

It is not clear whether part of the molecular material that encircles both the HI and HII shells participates in the expansion. An estimate of the amount of molecular gas can be obtained from Fig. 7 by applying the empirical relation between $W_{CO}(=\int T_{mb}dv)$ and the H_2 column density $N_{H_2} = (1.1\pm0.2)\times10^{20} \times W_{CO}$ cm^{-2}(K km s^{-1})$^{-1}$, obtained from γ-ray studies of molecular clouds in the IV galactic quadrant (Slane et al. 1999). The total H_2 mass is estimated to be 6800 M$_\odot$.

4.3 The energetics

An estimate of the mechanical luminosity L_w ($= \dot{M} V_w^2/2$) of the stellar wind of WR 85 can be obtained by assuming a typical mass loss rate $\dot{M} = 2\times10^{-5}$ M$_\odot$ yr^{-1} for the WN phase (Cappa et al. 2004) and a terminal velocity $V_w = 1430$ km s^{-1} (Rochowicz & Nieldzieski 1995). For the previous main sequence O-type star phase, we adopted $\dot{M} = 2\times10^{-6}$ M$_\odot$ yr^{-1} and a terminal velocity $V_w = 1000$ km s^{-1} (Prinja, Fullerton & Crowther 1996). Mechanical luminosities corresponding to the WR and the O-type star phases turn out to be $L_{WR} = 1.3\times10^{37}$ erg s^{-1} and $L_O = 6.3\times10^{35}$ erg s^{-1}. Assuming a typical lifetime for the WN phase $t_{WN} = 0.3\times10^6$ yr (Meynet & Maeder 2003) and for the O-type phase $t_O = 3\times10^6$ yr (Conti & Vacca 1990), the total stellar wind mechanical energy transferred to the ISM is $E_w = 1.8\times10^{50}$ erg. A similar value (1.2×10^{50} erg) is derived asuming that the stellar wind of the WR star and the previous O-type star phase have blown the gas bubble during 0.3×10^6 and 0.8×10^6 yr, respectively. These lifetimes are compatible with the derived dynamical age. Taking into account the large uncertainty in the dynamical age, we believe that the derived E_w-values can be considered as the lower and upper limits to the true stellar wind energy.

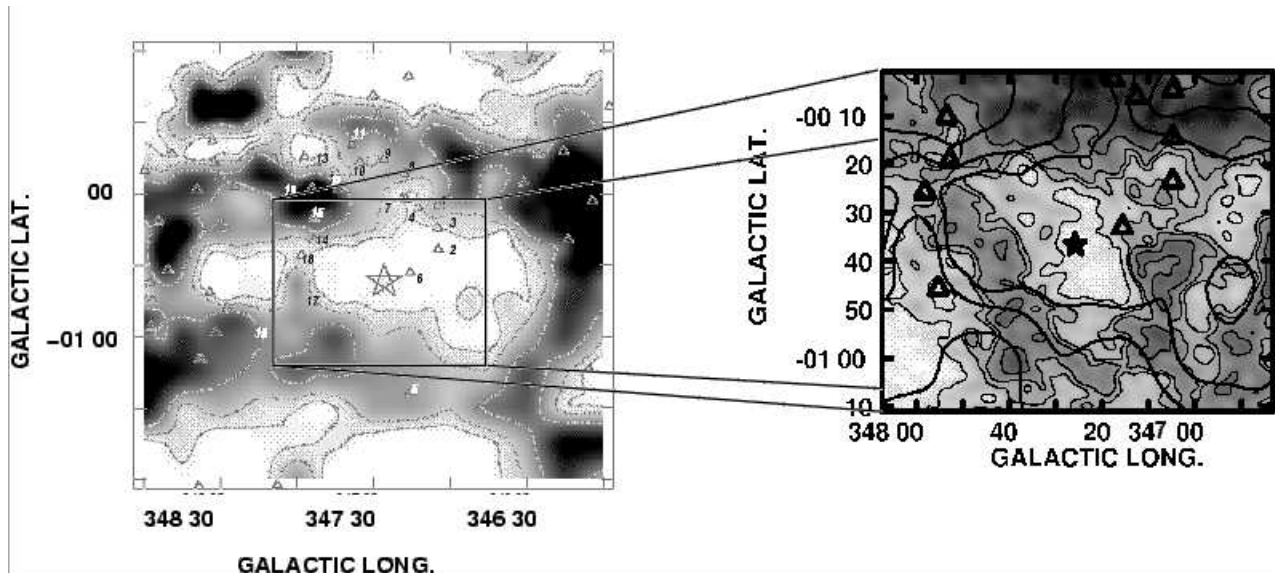The kinetic energy E_k ($= M_s V_{exp}^2/2$) in the interstellar

Figure 7. *Left panel:.* Mean brightness temperature corresponding to the CO emission distribution within the velocity interval –32.5 to –24.7 km s^{-1}. The grey scale corresponds to 0.2 to 1.7 K. The contour lines are 0.3, 0.5 and 0.9 K. The cross marks the position of the WR star. The triangles mark the location of IRAS protostellar candidates (see text). *Right panel:* Enlargement of the central region of the image on the left showing an overlay of the Hı (*grayscale and thin contour lines*) and the CO (*thick contour lines*) emissions. The star symbol indicates the stellar position. The triangles mark the location of IRAS protostellar candidates.

bubble derived taking into account the expansion velocity from Table 2 and the swept-up atomic neutral and ionized masses, is $E_k= 8.3\times10^{48}$ erg. If the molecular material also participates in the expansion, $E_k= 8.8\times10^{48}$ erg.

The ratio ϵ ($= E_k/E_W$) is in the range 0.005 - 0.03. These values indicate that the central star is capable of blowing the interstellar bubble. The figure derived for WR 85 is similar to the ones obtained for most of the Hı interstellar bubbles found around O- and WR-stars. These values support the interpretation that bearing in mind the standard energy conserving model by Weaver et al. (1977), the observed stellar wind energy appears to be too high for the observed bubble dynamics, as pointed out by Cooper et al. (2004), and suggest that the bubbles are most probably in the momentum conserving stage. However, the drain of energy from the bubble through the patchy envelope can not be ruled out.

The ambient density obtained by distributing the total mass within the volume of the bubble (see §4.2) is compatible with the value derived for the momentum conserving case (~ 3 cm^{-3}).

The SNR G 347.3-0.5 is seen projected onto the same area. The derived distance to the SNR, $d = 6$ kpc, based on molecular line information (Slane et al. 1999), precludes any relation between the SNR and RCW 118 and the Hı shell.

5   CONDITIONS FOR STAR FORMATION

The high velocity mass flow produces a drastic change in the physical conditions of the surrounding ISM. Shock fronts linked to stellar winds from massive stars may induce star formation in the high density regions of the neutral shells, where material has accumulated and conditions for star formation may have been favoured. Then, it is important to

analyze the presence of star formation indicators in the neutral shells.

Since protostellar candidates can be identified as infrared sources in the IRAS Point Source Catalogue, we performed a search for IRAS point sources projected onto a region of $3°$ in size centered at the stellar position whose energy distributions are compatible with protostellar objects according to the criteria listed by Junkes, Fürst & Reich (1992). The IR sources found in our search are indicated by triangles in Fig. 7 (left panel). Only the ones within an area of $1°$ in radius centered at the WR position (triangles with numbers) are listed in Table 3, which shows the source number, its IRAS number identification, and the fluxes in the four IRAS bands.

It is clear from the left panel of the figure that most of the sources are projected onto regions of strong CO emission or close to the galactic plane. The triangles in the right panel of Fig. 7 mark the position of IRAS point sources. This panel shows the close correspondence between the IR sources 2, 3, 6, 14, 15, 17 and 18, and the molecular and Hı shells linked to RCW 118, suggesting that sequential star formation may be occuring in some sections of the neutral envelope, where conditions for stellar formation might have been developed. We note that the distances to these sources are unknown.

6   SUMMARY

We have analyzed 21cm line data belonging to the Southern Galactic Plane Survey searching for an Hı bubble related to WR 85 and its ring nebula RCW 118. The main results of our search can be summarized as follows:

(i) The Hı data allowed the identification of a cavity in the neutral gas distribution surrounded by a slowly expanding shell. The structure was detected at velocities spanning the

Table 3. Protostellar candidates within a region of $1°$ in radius centered on WR 85

#	l	b	IRAS designation	F(12μm)	F(25μm)	F(60μm)	F(100μm)
	($°$ $'$)	($°$ $'$)	(Jy)	(Jy)	(Jy)	(Jy)	(Jy)
1	347 4	-0 4	17076-3940	3.75	3.82	131.	410.
2	347 4	-0 22	17089-3951	4.38	13.	98.5	234.
3	347 4	-0 13	17083-3946	7.94	4.42	39.70	182.
4	347 12	-0 6	17081-3935	2.75	4.13	94.5	435.
5	347 15	-1 22	17137-4018	18.89	7.55	63.5	188.
6	347 15	-0 33	17101-3948	3.25	4.57	18.70	64.59
7	347 17	-0 1	17081-3928	11.	74.30	221.	739.
8	347 17	0 8	17074-3922	3.78	7.38	256.	1120.
9	347 25	0 13	17074-3911	4.69	2.42	150.	397.
10	347 34	0 12	17079-3905	57.20	396.	4030.	8220.
11	347 38	0 20	17076-3858	2.67	4.03	80.80	280.
12	347 43	0 1	17091-3905	62.20	24.89	37.5	211.
13	347 45	0 9	17087-3859	4.00.	25.10	245.	628.
14	347 52	-0 18	17110-3910	3.43	18.29	221.	941.
15	347 52	-0 10	17105-3904	1.60	9.10	91.69	226.
16	347 53	0 2	17096-3856	24.00	164.00	1050.	1720.
17	347 55	-0 45	17130-3923	3.49	21.90	145.	148.
18	347 58	-0 25	17118-3909	9.72	80.30	1120.	3000.
19	348 13	-0 58	17149-3916	209.	988.	6760.	9160.

interval –28.0 to –16.5 km s^{-1}, and has a systemic velocity of –21±5 km s^{-1}. The cavity can also be identified in the CO emission distribution at similar velocities.

(ii) The ring nebula RCW 118 appears projected onto the inner border of the H I shell.

(iii) The systemic velocity of the H I structure is similar to the velocity of the ionized gas in RCW 118.

(iv) WR 85 is seen in projection onto the central part of the H I cavity and close to its geometrical center.

(v) The coincidence, within errors, of the kinematical distance to the H I structure and the stellar distance strongly suggests that the WR star is placed within the cavity.

(vi) The morphological coincidence between the inner optical nebula and the H I emission at about –28 km s^{-1} suggests that the 9ʹ3 nebula is located on the approaching part of the expanding shell. The WR star, which appears closely related to the inner nebula, is also probably located near the approaching part of the shell.

(vii) The CO emission distribution reveals the presence of a molecular shell almost encircling the HI envelope.

(viii) The position of the IRAS protostellar candidates projected onto the molecular shell, suggests that star formation might be occuring in the region. However, additional studies should be performed to investigate this point.

(ix) The stellar wind of WR 85 is capable of blowing the observed ionized and neutral structure.

The bulk of evidence (i) to (ix) strongly indicates that the H I structure is the neutral gas counterpart of the optical bubble and shows the action of the stellar winds on the surrounding material.

Adopting a distance of 2.8±1.1 kpc, the neutral interstellar bubble has a linear radius of ∼21 pc. Taking into account an expansion velocity of 9±2 km s^{-1}, its dynamical age is 1.1×10^6 yr, suggesting that both the present WR star and its massive stellar progenitor have contributed in shaping the bubble. The associated neutral and ionized masses are 3000 M$_\odot$, which indicates that the bubble evolved in a medium with an average ambient density of 3 cm^{-3}.

REFERENCES

Brand J., Blitz L. 1993, A&A, 275, 67
Cappa C., Goss W. M., van der Hucht K. A., 2004, AJ, 127, 2885
Cappa C., Arnal M., Cichowolski S., Goss W.M., Pineault S. 2003, IAU Symp. 212, A Massive star Odyssey, from Main Sequence to Supernova, p. 596
Cappa C., Goss W. M., Pineault S., 2002, AJ, 123, 3348
Chu Y.-H., Treffers R. R., Kwitter K. 1983, ApJS, 53, 937
Chu, Y.-H., Treffers, R. R. 1981, ApJ, 250, 615
Condon J. J., Broderick J. J., Seielstad G. A., 1995, ADIL, JC, 6
Conti P. S., Vacca W. D. 1990, AJ, 100, 431

Cooper R. L., Guerrero M. A., Chu Y. -H., Rosie Chen C. -H., Dunne B. C., 2004, ApJ, 605, 751

Dame T. M., Hartmann D., Thaddeus P. 2001, ApJ, 547, 792

Duncan, A. R., Stewart R. T., Haynes R. F., Jones K. L. 1995, MNRAS, 277, 36

Gaustad J. E., McCullough P. R., Rosing W., Van Buren D. 2001, PASP, 113, 1326

García-Segura, G., Mac Low, M.-M. 1995, ApJ, 455, 145

Georgelin, Y. M., Georgelin, Y. P. 1976, A&A, 49, 57

Haynes R. F., Caswell J. L., Simons L. W. J, 1978, AuJPA, 45, 1

Heckathorn, J. N., Bruhweiler F. C., Gull T. R. 1982, ApJ, 252, 230

Hunter S.D., Digel S.W., de Geus E.J., Kanback G., 1994, ApJ, 436, 216

van der Hucht K. 2001, New astronomy Rev., 45, 135

Junkes N., Fürst E., Reich W., 1992,A&AS, 261, 289

Lamers H.J.G.L.M., Leitherer C., 1993, ApJ, 412, 771

Lazendic J. S., Slane P. O., Gaensler B. M., Reynolds S. P., Plucinsky P. P., Hughes, J. P., 2004, ApJ, 602, 271

Leitherer C, Chapman J.M., Koribalski B., 1997, ApJ, 481, 898

Marston A.P., Yocum D. R., García-Segura G., Chu, Y.-H. 1994a, ApJS, 93, 229

Marston A.P., Yocum D. R., García-Segura G., Chu, Y.-H. 1994b, ApJS, 95, 151

Mathis J.S., Cassinelli J. P., van der Hucht K. A., Prusti T., Wesselius P. R., Williams P. 1992, ApJ, 384, 197

McClure-Griffiths N. M., Dickey J. M., Gaensler B. M., Green A. J., Haverkorn M., Strasser S., 2005, ApJ, in press.

McCray R., 1983, HiA, 6, 565

Meynet G., Maeder A. 2003, A&A, 404, 975

Mezger P. G., Henderson A. P., 1967, ApJ, 147, 471

Moffat A.F.J., Fitzgerald M.P. 1977, A&A, 54, 263

Pfeffermann E., Aschenbach B., 1996, rftu.proc., 267

Prinja R.K., Barlow M.J., Howarth I.D., 1990,ApJ, 361, 607

Prinja R.K., Fullerton A.W., Crowther P.A., 1996, A&A, 331, 264

Rochowicz K., Nieldzieski A., 1995, AcA, 45, 307

Slane P., Gaensler B. M., Dame T. M.,Hughes J. P., Plucinsky P. P., Green A., 1999, ApJ, 525, 357

Weaver R., McCray R., Castor J., Shapiro, P., Moore R., 1977, ApJ, 218, 377